Covariance Differencing and Higher Order Cumulant Methods for DOA Array Processing in the Presence of Colored Noise Fields

Nate Golding {nathan.golding@colorado.edu}

Dept. of Electrical, Computer, and Energy Engineering
University of Colorado at Boulder

Submitted in partial fulfillment of the requirements of
ECEN 5244 Stochastic and Environmental Signal Processing

***Abstract*— Subspace methods for direction of arrival estimation such as Multiple SIgnal Classification (MUSIC) are common due to their high accuracy and computational efficiency, however the standard assumptions of spatially and temporally white noise degrade the performance. Methods for mitigating colored noise such as covariance transformation differencing and higher order cumulants have been suggested and researched for the purpose of handling colored noise fields. In this paper, we investigate the performance differences in the presence of various levels of colored noise across signal to noise ratio (SNR).**

I. INTRODUCTION

The Multiple SIgnal Classification (MUSIC) algorithm, introduced by Schmidt [1], is a method for estimating the directions of arrival (DOA) from multiple emitters incident on a sensor array, and after its introduction quickly became one of the most popular forms of DOA estimation. MUSIC uses eigendecomposition of the sensor covariance matrix, separating the signal and noise into orthogonal subspaces in order to search the angle of incidence space for vectors which are maximally orthogonal to the noise subspace. As such, the algorithm becomes highly sensitive to non-idealities in the covariance matrix, namely highly or fully correlated (or *coherent*) signals and colored noise. Much research has been put into the handling of coherent signals, such as occurs in multipath environments, such as spatial smoothing with forward and backward subarray techniques [2], [3], and more recently with subspace and wavelet smoothing techniques [4], [5]. The focus of this paper is on methods of handling cases of correlated and spatially colored noise, namely covariance array differencing and higher order cumulant processing. While the authors of the relevant previous works on these techniques provide simulation examples, their tests typically choose a single value for SNR, and exclude performance in cases where their assumptions may not hold. In this paper we introduce the relevant DOA techniques and simulate their performance across varying noise fields against SNR and integration time in terms of steady state bearing resolution error statistics.

II. BACKGROUND

Direction of Arrival (DOA) estimation involves determining the angles at which signals arrive at an array of sensors, such as antennas or microphones. It is widely used in fields like radar, wireless communications, and acoustics to enable beamforming, target localization, and interference mitigation. MUSIC exists in a field of DOA estimation techniques which include monopulse and ESPRIT, and although more computationally intensive, the MUSIC algorithm attains increased spatial resolution and tolerance to noise in comparison to many techniques.

A. Standard MUSIC DOA

Consider a 1-dimensional uniform linear array (ULA) of sensor elements. The array consists of M identical isotropic sensors, each separated by a distance d, upon which there are N incident narrow-band signals approximated at frequency f_c arriving from N separate sources, each having an angle of arrival θ_k defined with reference to bore sight (90° from horizon). The signals are considered to be far-field, and are treated as plane waves. From the geometry of the system it is evident that the k-th wavefront travels an additional $d\cos(\theta_k)$ between neighboring sensors, contributing a time difference of $d\cos(\theta_k)/c$, and a phase difference of $2\pi d\cos(\theta_k)/c$. For convenience, we define $a(\theta_k) = \exp\{-j2\pi\frac{d}{\lambda}\cos(\theta_k)k\}$, which can be considered as the arrival or steering vector of the k-th wavefront. With reference to the first (leftmost) element of the array, the signal received by sensor i at time t is

$$x_i = \sum_{k=0}^{N} s_k(t)a(\theta_k) + n_i(t) \tag{1}$$

where $s_k(t)$ is the signal transmitted by the k-th source, λ is the source signal wavelength, and $n_i(t)$ is the additive noise on sensor i at time t. In vector notation, equation 1 becomes

$$x(t) = As(t) + n(t) \tag{2}$$

Under the assumption of signals which are uncorrelated to the noise, and the noise is spatially white, the array

covariance matrix is

$$\begin{aligned} R_{xx} &= E[X(t)X^{\dagger}(t)] \\ &= AR_{ss}A^{\dagger} + \sigma_n^2 I \end{aligned} \tag{3}$$

where R_{ss} the covariance matrix of the signal sources defined by $E[s(t)s^{\dagger}(t)]$.

So long as $d \leq \lambda/2$, all of the columns of A are different, and because A has a Vandermonde structure, i.e. the columns of A have the form $\begin{bmatrix} 1 & a(\theta) & a^2(\theta) & \dots & a^M(\theta) \end{bmatrix}$, they must also be linearly independent as they each form a unique M-th order polynomial. So long as R_{ss} is non-singular, which is true when the source signals are not coherent, the rank of $AR_{ss}A^{\dagger}$ must be equal to the rank of R_{ss} which is N. In the noiseless case, this means that the array covariance R_{xx} has N non-zero eigenvalues, whose eigenvectors $E_s = [v_1, \dots, v_N]$ span the *signal subspace*, and $M - N$ zero eigenvalues, whose eigenvectors $E_n = [u_{N+1}, \dots, u_M]$ span the *null subspace*. Notably, the columns of A also span the signal subspace, meaning that $A^{\dagger}u_i = 0 \ \forall u_i \in E_n$. When noise is added, all of the eigenvalues increase by the noise power and the arrival vectors remain orthogonal to the *noise subspace*. A more formal treatment of the above is shown by Schmidt [1].

The above provides the basis for the DOA estimation, which is performed by maximizing the MUSIC psuedospectrum:

$$P_{MUSIC}(\theta) = \frac{1}{a^{\dagger}(\theta)E_nE_n^{\dagger}a(\theta)} = \frac{1}{\|E_n^{\dagger}a(\theta)\|^2} \tag{4}$$

which is equivalent to finding the angles of arrival which are maximally orthogonal to the noise subspace. Since $A^{\dagger}u_i \approx 0$, $P_{MUSIC}(\theta^*) \approx \infty$ for θ^* being one of the true incident bearings.

B. Colored Noise Fields

In the derivation of the MUSIC algorithm, the noise is assumed to be spatially white – zero mean, equal in power, and uncorrelated between elements. In real sensor arrays, equal noise power across channels is unrealistic, and the assumption of uncorrelated noise is questionable when mutual inductance between array elements are significant, or when the receivers have low noise figures. Torrieri and Bakhru [6] quantify the effects of spatially colored noise on the MUSIC and reduced MUSIC algorithms via simulation, finding that unequal noise power and correlated noise lead to steady state bias in resolved angles, fluctuations in said steady state, and a drastically increased convergence time, especially as SNR decreases beyond 10dB. As such, methods for handling spatially colored noise are highly desirable.

C. Covariance Differencing

The essence behind covariance differencing techniques is as follows. Consider the array covariance matrix R_{xx} in equation 3. If we did not assume spatially white noise, we instead have

$$R_{xx} = AR_{ss}A^{\dagger} + R_{nn} \tag{5}$$

where R_{nn} is likely unknown and difficult to estimate accurately. Covariance differencing circumvents this problem by providing two covariance matrices in which the signal subspace is meaningfully transformed, but the noise subspace is left constant, and then subsequently differencing the two covariance matrices to suppress the effects of noise without suppressing the signals.

1) Multiple Measurement Approach: As Paulraj and Kailath discussed in [7], two array covariance matrices can be obtained by taking two measurements with some transformation. Transformations can be spatial, such as rotations and translation of the array, or temporal. For example, noise is invariant to rotational transformations in the case where the noise is primarily contributed by the array platform, while the signal's arrival vectors will be altered, changing the signal covariance. The use of a temporal transformation depends on the noise being long-term stationary, while the signals are only short-term stationary.

The new array covariance is described by the difference of the array covariance of the two measurements, R_1,R_2

$$\begin{aligned} P &= R_1 - R_2 \\ &= \begin{bmatrix} A_1 & A_2 \end{bmatrix} \begin{bmatrix} R_{ss,1} & 0 \\ 0 & R_{ss,2} \end{bmatrix} \begin{bmatrix} A_1 & A2 \end{bmatrix}^{\dagger} \end{aligned} \tag{6}$$

As shown in [7], in the treatment of transformations in which $A_1 \neq A_2$, for example in a rotational transformation, if the columns of $\begin{bmatrix} A_1 & A2 \end{bmatrix}$ are unique and $R_{ss,1}$, $R_{ss,2}$ are non-singular, P will have $M - 2N$ zero eigenvalues, which have corresponding eigenvectors orthogonal to the columns of $\begin{bmatrix} A_1 & A2 \end{bmatrix}$. The rank of P is

$$\begin{aligned} \rho(P) &= \rho(\begin{bmatrix} A_1 & A_2 \end{bmatrix} \begin{bmatrix} R_{ss,1} & 0 \\ 0 & R_{ss,2} \end{bmatrix} \begin{bmatrix} A_1 & A_2 \end{bmatrix}^{\dagger}) \\ &= \rho(\begin{bmatrix} R_{ss,1} & 0 \\ 0 & R_{ss,2} \end{bmatrix}) = 2N \end{aligned} \tag{7}$$

Given equation 7, it is shown that the subspace spanned by the eigenvectors corresponding to the non-zero eigenvalues is the same subspace as is spanned by the direction vectors of A_1, A_2.

Forming the MUSIC psuedospectrum requires application specific information. Consider the case of rotational transformation, such that every arrival vector $a(\theta_k) \in A_1$ has a corresponding arrival vector $a(\theta_{k+\alpha}) \in A_2$, where α is the rotation applied to the array plane between covariance measurements. Here the psuedospectrum is

$$P_{MUSIC} = \frac{1}{\|E_n^{\dagger}a(\theta)\|^2 + \|E_n^{\dagger}a(\theta + \alpha)\|^2} \tag{8}$$

where E_n are the noise subspace eigenvectors of the differenced array covariance matrix P.

2) Linear-Transformation Approach: The multiple measurement approach depends temporal stationarity, and typically a rotation or translation which may not be practical. Prasad *et al* [8] proposed a method using linear transformations on a single measurement, given *a priori* information about the structure of the noise covariance matrix R_{nn}. Prasad *et al* focus on a structure which assumes spatially

stationary, but correlated noise – ie a Hermitian symmetric Toeplitz matrix.

Symmetric Toeplitz matrices are invariant under the transformation

$$\begin{bmatrix} 0 & \cdots & & 1 \\ & & 1 & \\ & \cdots & & \\ 1 & & & \end{bmatrix} R_{nn} \begin{bmatrix} 0 & \cdots & & 1 \\ & & 1 & \\ & \cdots & & \\ 1 & & & \end{bmatrix} \tag{9}$$

leading to the array covariance difference

$$\begin{aligned} P &= R_{xx} - JR_{xx}J \\ &= AR_{ss}A^\dagger - JAR_{ss}A^\dagger J \\ &= \begin{bmatrix} A & JA \end{bmatrix} \begin{bmatrix} R_{ss} & 0 \\ 0 & -R_{ss} \end{bmatrix} \begin{bmatrix} A & JA \end{bmatrix}^\dagger \end{aligned} \tag{10}$$

Proof that the new covariance upholds signal/noise subspace orthogonality is covered in [8]. As with the multiple measurement approach, when applying equation 4 there are two sets of N bearings, one which comes from A and the other which comes from JA corresponding to the negatives of the true bearings.

Paulraj *et al* [7] introduce a method for separating these "phantom" bearings. The arrival vectors for the $2N$ resolved angles are collected into a $M \times 2N$ matrix, in no particular order.

$$A_{12} = \begin{bmatrix} a(\theta_1) & \dots & a(\theta_{2N}) \end{bmatrix} \tag{11}$$

From this, the permuted signal covariance matrix $R_{ss,12}$ can be derived as

$$\begin{aligned} P &= A_{12}R_{ss,12}A_{12}^\dagger \\ R_{ss,12} &= (A_{12}^\dagger A_{12})^{-1}A_{12}^\dagger P A_{12}(A_{12}^\dagger A_{12})^{-1} \end{aligned} \tag{12}$$

The signs of the real parts of the diagonal elements of $R_{ss,12}$ are used to order the bearings into the two groups corresponding to the real and phantom angles.

Moghaddamjoo [9] discusses a similar process, now in the case where the structure is not Toeplitz, but rather non-uniform diagonal, ie the uncorrelated case with unequal power noise across sensors. The transform suggested by Moghaddamjoo is one of the form in equation 13,

$$J = \begin{bmatrix} 1 & & & & 0 \\ & \rho & & & \\ & & \rho^2 & & \\ & & & \ddots & \\ 0 & & & & \rho^{M-1} \end{bmatrix} \tag{13}$$

which is applied to get the difference covariance matrix

$$\begin{aligned} P &= j(JR_{yy}J^{-1} - J^{-1}R_{yy}J) \\ &= j(JAR_{ss}A^\dagger - J^{-1}AR_{ss}A^\dagger J) \\ &= \begin{bmatrix} JA & J^{-1}A \end{bmatrix} \begin{bmatrix} 0 & jR_{ss} \\ -jR_{ss} & 0 \end{bmatrix} \begin{bmatrix} JA & J^{-1}A \end{bmatrix}^\dagger \end{aligned} \tag{14}$$

Equation 14 assumes R_{nn} is assumed to be diagonal, meaning the effects J and J^{-1} negate each other such that $JR_{nn}J^{-1} = J^{-1}R_{nn}J = R_{nn}$. The effect of the transformation on the direction vectors Ja_i and $J^{-1}a_i$ have a Vandermonde structure, and so long as all incident direction angles are unique, both JA and $J^{-1}A$ are both full rank such that the direction vectors from each span $\mathbb{C}^M$. This results in $2M$ non-zero eigenvalues, and $N - 2M$ null eigenvalues. The psuedospectrum searches for maximum orthogonality to the null subspace for both $Ja(\theta_i)$ and $J^{-1}a(\theta_i)$, resulting in equation 15.

$$P_{MUSIC} = \frac{1}{\|E_n^\dagger Ja(\theta)\|^2 + \|E_n^\dagger J^{-1}a(\theta)\|^2} \tag{15}$$

D. Higher Order Cumulants

Porat and Friedlander [10] introduce a method of MUSIC which uses fourth order cumulants in the place of covariance. Cumulants of degree higher than 2 have the benefit that Gaussian processes are zero, meaning that Gaussian noise is completely suppressed in the DOA estimate with no *a priori* knowledge of the noise covariance. It is important to note that the signals must be non-Gaussian, or else they too will be suppressed.

For the second order moment (covariance) defined by

$$\mu_2(k,l) = E[y_k(t)y_l^*(t)] \tag{16}$$

and fourth order moment (kurtosis) defined by

$$\mu_4(k_1,k_2,l_1,l_2) = E[y_{k_1}(t)y_{k_2}(t)y_{l_1}^*(t)y_{l_2}^*(t)] \tag{17}$$

the fourth order cumulant can be given by

$$\begin{aligned} \kappa_4(k_1,k_2,l_1,l_2) = \mu_4(k_1,k_2,l_1,l_2) \\ - \mu_2(k_1,l_1)\mu_2(k_2,l_2) \\ - \mu_2(k_1,l_2)\mu_2(k_2,l_1) \end{aligned} \tag{18}$$

The fourth order cumulant matrix can be formed using Kronecker products ($\otimes$) as

$$C = (A \otimes A^*)S(A \otimes A^*)^\dagger \tag{19}$$

which is an M^2xM^2 matrix for the 4th order cumulant matrix of $s(t)$:

$$\begin{aligned} S = E[(s(t) \otimes s^*(t))(s(t) \otimes s^*(t))^\dagger] \\ -E[s(t) \otimes s^*(t)]E[(s(t) \otimes s^*(t))^\dagger] \\ -E[s(t)s^\dagger(t)] \otimes E[s(t)s^\dagger(t)] \end{aligned} \tag{20}$$

For statistically independent (incoherent) sources, the matrix C will have $M^2 - N^2$ zero eigenvalues, with the rest being non-zero, but potentially negative. With singular value decomposition,

$$C = \begin{bmatrix} U_1 & U_2 \end{bmatrix} \begin{bmatrix} \Lambda & 0 \\ 0 & 0 \end{bmatrix} \begin{bmatrix} V_1^\dagger \\ V_2^\dagger \end{bmatrix} \tag{21}$$

The columns of matrix $(A \otimes A^*)$ are orthogonal to the columns of U_2, i.e. the vectors which span the null subspace, meaning we can define the psuedospectrum as

$$P_{MUSIC} = \frac{1}{\|(a(\theta) \otimes a^*(\theta))^\dagger U_2\|^2} \tag{22}$$

The primary benefit of 4th order statistics over the traditional second order is Gaussian noise suppression. Although outside the scope of the works of this paper, Dogan and Mendel [11] introduce a study of the effects of non-Gaussian noise on 4th order cumulant methods in DOA estimation and propose methods of non-Gaussian noise suppression with 4th order cumulants.

III. METHODS

The goal of this study is to investigate the performance of the aforementioned modified MUSIC algorithms against SNR and integration time for varying noise fields.

A. MUSIC Algorithms

The studied algorithms include standard MUSIC [1], covariance differencing under Toeplitz and diagonal noise covariance assumptions [8][9], and 4th order cumulants method [10]. These will be referred to as standard MUSIC, Toeplitz Differencing MUSIC, Diagonal Differencing MUSIC, and Cumulant MUSIC respectively. The algorithms are implemented in the mathematical forms discussed in section II, despite options for greater computational performance, as the focus is on analysis of the limits of statistical performance rather than computational performance. For detailed information on the implementation of the algorithms code for all algorithms and analytics can be found on GitHub [13], where they are implemented in Python with Numpy, SciPy, and Matplotlib [14][15][16].

B. Noise Covariance Structures

The noise fields which are studied are defined by the structure of the noise covariance matrices. The relevant structures used include the following: a uniform diagonal structure, corresponding to the ideal case of uncorrelated noise of equal power across all sensors; a non-uniform diagonal strucutre, corresponding to the case of uncorrelated noise of unequal power across sensors; a block diagonal structure, corresponding to the case of correlated noise such that closer sensors are correlated, as in the case of correlated noise caused by coupling in the receiver; a symmetric Toeplitz structure, corresponding to the case of correlated noise of equal power across sensors, as may occur when receiver noise figures are very low, and noise sources may be off-platform; and a symmetric non-Toeplitz structure, corresponding to the case of correlated noise of unequal power across sensors, as may occur when a mix of the above situations are equally relevant.

The prescribed covariance matrices are obtained by eigendecomposition of the desired matrix and a set of normally distributed random variables [12]:

$$R_{nn} = E\Lambda E^{\dagger}$$
$$x(t) = E(\Lambda)^{\frac{1}{2}} \begin{bmatrix} n_1(t) \\ n_2(t) \\ \vdots \\ n_M(t) \end{bmatrix} \tag{23}$$

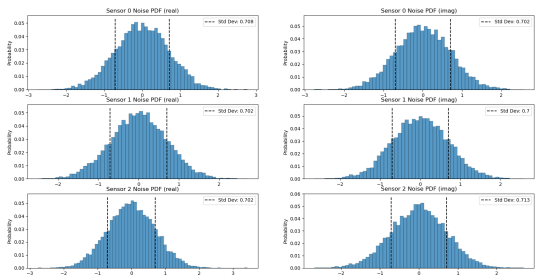

Fig. 1. Real/Imaginary noise probability density functions. Real and imaginary components have zero mean standard deviation 0.707, equaling complex-valued signals with power 1.

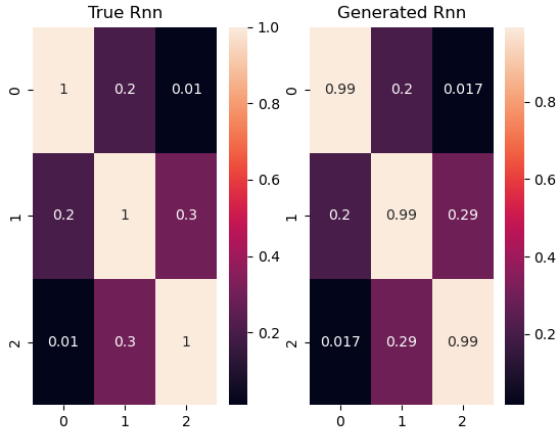

Fig. 2. Example of prescribed noise covariance and eigenvalue-generated noise covariance matrices for a 3-sensor ULA.

where n_m are normally distributed random processes, E are the eigenvectors and Λ the eigenvalues of the noise covariance matrix, and $x(t) \in \mathbb{C}^M$ the noise random process having prescribed covariance.

As an example, Figures 1 and 2 show the PDFs and covariance matrices of the generated noise for an arbitrary noise covariance over 1024 samples.

C. Metrics

The performance of the algorithms is discussed in terms of bearing resolution error statistics. Given that there are multiple bearings estimated on any given algorithm step, the analyzed statistics are the expected value and standard deviations of error across all resolved angles at each step. For example, if the true angles are $\begin{bmatrix}\theta_1 & \dots & \theta_N\end{bmatrix}$, and the algorithm yields bearing estimates $\begin{bmatrix}\hat{\theta}_1 & \dots & \hat{\theta}_N\end{bmatrix}$, then the expected error and error standard deviation are defined as

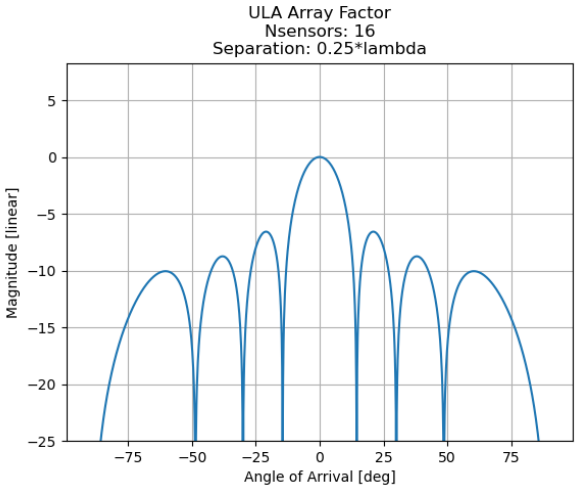

Fig. 3. 16-element, $\lambda/2$ Spacing ULA Array Factor

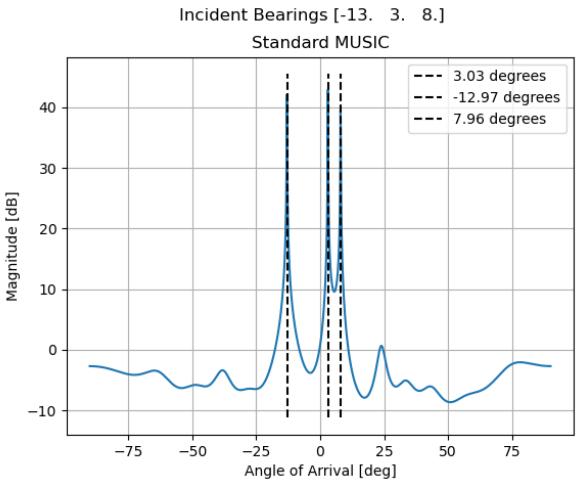

Fig. 4. Standard MUSIC psuedospectrum at 20dB SNR, uniform diagonal noise covariance, 1024 samples. Resolved bearings are [-12.97, 3.03, 7.96] with true bearings [-13, 3, 8].

$$E[\cdot] = \sum_{i=1}^{N} |\theta_i - \hat{\theta}_i|$$
$$\sigma = \sqrt{\sum_{i=1}^{N} (\theta_i - \hat{\theta}_i)^2} \tag{24}$$

These error statistics are analyzed for varying SNR values, integration times, i.e. the number of samples per resolution step, and the structure of the noise covariance matrix. In section IV, the algorithms are often said to converge at a particular SNR or integration time. Formally, this is treated as when an algorithm's expected error reaches $E[\cdot] \leq 2^\circ$ and remains there.

D. Array Configuration

The ULA is configured with 16 isotropic antenna elements separated by half-wavelength intervals, with no weighting or steering applied. Such a configuration is typical for DOA applications, and is chosen for a balance of spatial resolution, sidelobe and grating lobe levels, and computational complexity. The array factor of is depicted in figures 3 showing main lobe half-power beamwidth (HPBW) of 8° and null-to-null beamwidth of 16°. In order to avid unintentional nulling and signal degradation, the input arrival angles are restricted to the main lobe, and so are always in the range $[-15^\circ, 15^\circ]$.

IV. RESULTS

A. Ideal Bearing Resolutions

To start, the algorithms are analyzed at high SNR of 20dB with the ideal assumption of a uniform diagonal noise covariance matrix $R_{nn} = \sigma_n^2 I_{M\times M}$. A set of three signals of unit power with bearings $[-13^\circ, 3^\circ, 8^\circ]$ are incident on the array, which captures 1024 samples for use in bearing estimation.

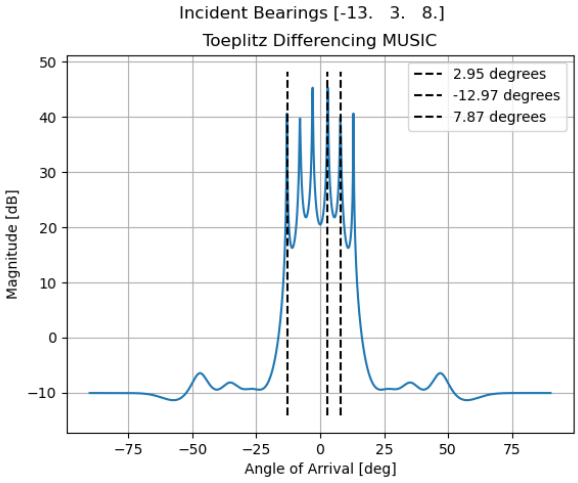

Fig. 5. Toeplitz Differencing MUSIC psuedospectrum at 20dB SNR, uniform diagonal noise covariance, 1024 samples. Resolved bearings are [-12.97, 2.95, 7.87] with true bearings [-13, 3, 8].

1) Standard MUSIC: The array covariance R_{yy} eigenvalue matrix contains three non-zero eigenvalues corresponding to the three incident signals and 13 near-zero eigenvalues corresponding to the noise subspace. The psuedospectrum is shown in figure 4 having sharp peaks at -12.97°, 7.96°, and 3.03°.

2) Toeplitz Differencing MUSIC: The array covariance eigenvalue matrix now has the three non-zero eigenvalues corresponding to the incident signals repeated, such that there are now 10 near-zero noise eigenvalues. Consequently, the pseudospectrum in figure 5 has six sharp peaks, corresponding to the true bearings [-13, 3, 8] and their negatives [13, -3, 8]. Using the bearing-grouping method discussed in equation 12, the estimated angles are -12.97°, 2.95°, and 7.87°.

3) Diagonal Differencing MUSIC: The array covariance eigenvalue matrix consists of 6 non-zero eigenvalues corresponding to the direction vectors from JA and $J^{-1}A$,

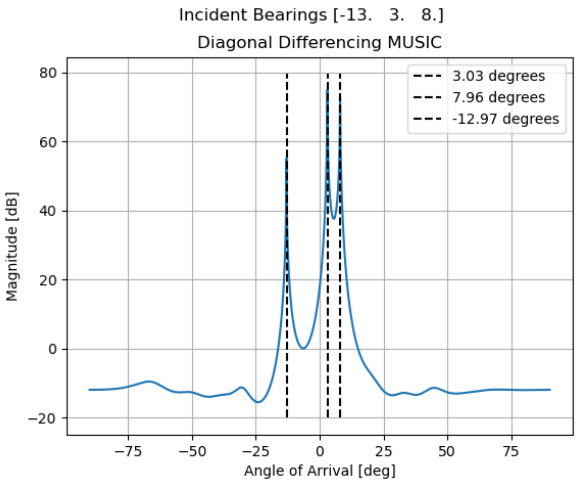

Fig. 6. Diagonal Differencing MUSIC psuedospectrum at 20dB SNR, uniform diagonal noise covariance, 1024 samples. Resolved bearings are [-12.97, 3.03, 7.96] with true bearings [-13, 3, 8].

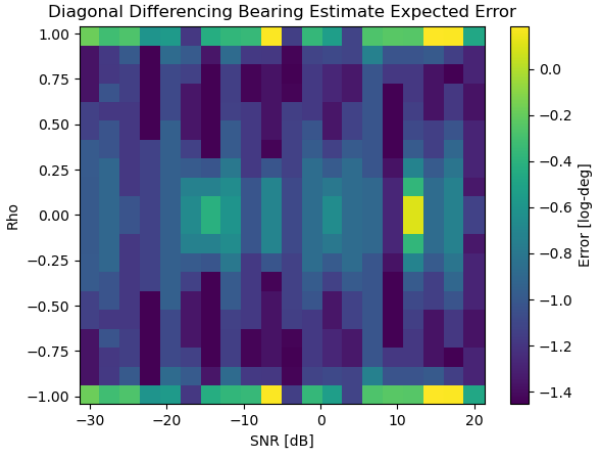

Fig. 7. Diagonal Differencing MUSIC angle estimation expected error ($\log_{10}$) vs SNR (in decibels) and metaparameter ρ.

and 10 near-zero eigenvalues corresponding to noise. The psuedospectrum depicted in figure 6 yields sharp peaks at bearings $-12.97°$, $3.03°$, and $7.96°$. Of all the methods, this algorithm yields the highest peak value near 80dB, compared to the more typical 50dB of the other algorithms. The diagonal differencing technique is unique in that it requires an additional meta-parameter ρ. The original paper [9] suggests the optimal values are $0.95 \leq |\rho| \leq 1$, from initial testing, this did not appear to be the case with our implementation. In order to determine the optimal value, the algorithm's error was evaluated against various values of ρ vs SNR. The results of this testing are shown in figure 7, which reveals that the most consistently optimal ρ value is near 0.75. From now on, the reader is to assume that $\rho = 0.75$.

4) Cumulants MUSIC: The array cumulants eigenvalue matrix contains 18 non-zero eigenvalues. The covariance matrix has dimension $M^2 \times M^2$, meaning 9 of the non-zero eigenvalues correspond to the true bearings. The other

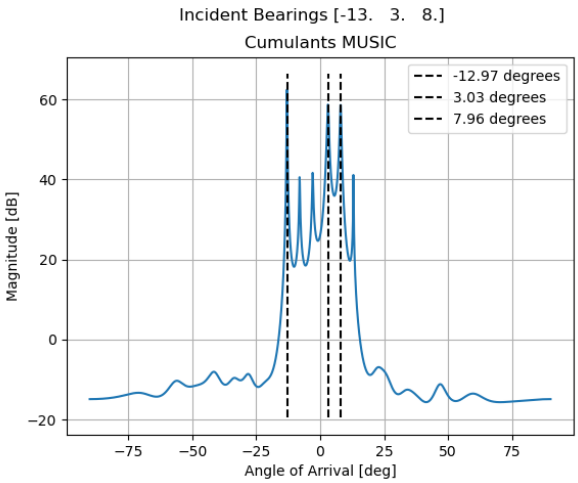

Fig. 8. Cumulants MUSIC psuedospectrum at 20dB SNR, uniform diagonal noise covariance, 1024 samples. Resolved bearings are [-12.97, 3.03, 7.96] with true bearings [-13, 3, 8].

9 non-zero eigenvalues correspond to the negatives of the true bearings. Using the same method for bearing-grouping as Toeplitz MUSIC, the correct angles are selected from their negative counterparts. This is apparent in the psuedospectrum shown in figure 8, which gives estimated angles $-12.97°$, $2.95°$, and $7.87°$.

B. Uniform Diagonal Noise Covariance

At some point, the algorithm's ability to resolve accurate bearings is reduced. Maintaining the same configuration of three incident signals with unit power and bearings $[-13°, 3°, 8°]$ with covariance approximated over 1024 samples, the algorithm's expected error and error standard deviation is evaluated over a range of SNRs from -30dB to 20dB. All algorithms are compared in figures 9 and 10. For the given configuration, standard MUSIC converges to near-zero error at -10dB, diagonal differencing at -4dB, Toeplitz differencing at 0dB, and cumulants at 4dB.

Considering now how the number of samples affects the convergence, the array is configured to -10dB SNR with the same signals used previously and evaluated for the number of samples from 10 to 1,000,000. The algorithm's expected error and error standard deviation are compared in figures 11 and 12, revealing standard MUSIC converging at 500 samples, diagonal differencing just over 1000 samples, Toeplitz differencing at 10,000 samples, and cumulants at a value greater than 1,000,000 samples. From these results, it is clear that the standard algorithm performs the best given a uniform diagonal noise covariance, both in terms of minimum SNR and minimum integration time.

C. Non-uniform Diagonal Noise Covariance

The uniform diagonal covariance structure requires only the noise variance σ_n^2 to be fully formed, however for a non-uniform diagonal structure, there are M different values for σ_n^2 which need to be considered. The non-uniform diagonal structure is formed by sampling the noise variances from a

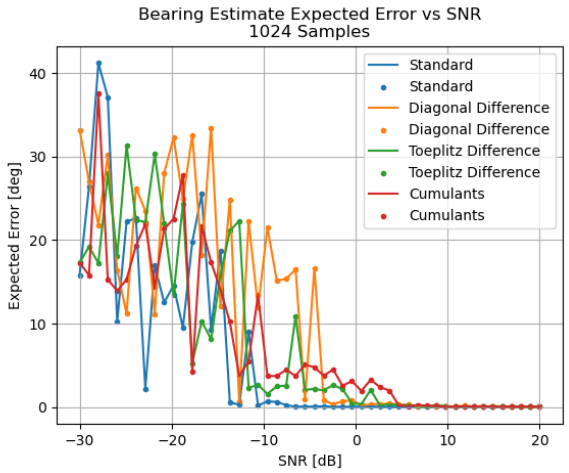

Fig. 9. Expected bearing estimation error vs SNR shown for all algorithms for 1024 samples and bearings [-13, 3, 8] and uniform diagonal noise covariance.

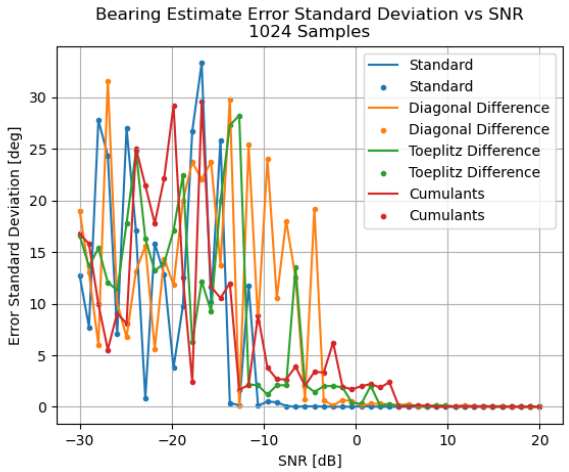

Fig. 10. Estimation bearing error standard deviation vs SNR shown for all algorithms for 1024 samples and bearings [-13, 3, 8] and uniform diagonal noise covariance.

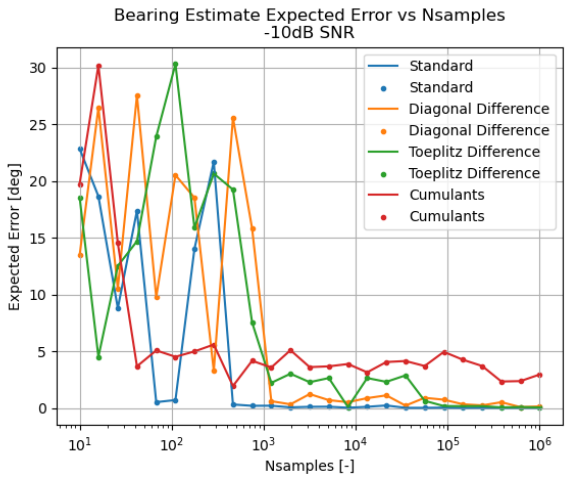

Fig. 11. Expected bearing estimation error vs integration time (number of samples) shown for all algorithms for -10dB SNR and bearings [-13, 3, 8] and uniform diagonal noise covariance.

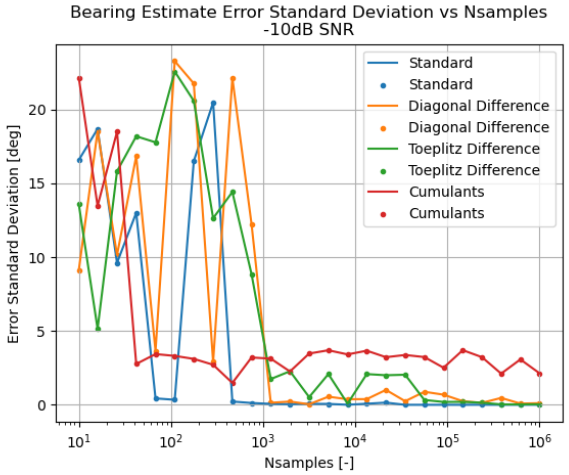

Fig. 12. Estimation bearing error standard deviation vs integration time (number of samples) shown for all algorithms for -10dB SNR and bearings [-13, 3, 8] and uniform diagonal noise covariance.

uniform distribution defined over the range $[\sigma^2_{n,max}, \sigma^2_{n,min}]$, with the added intricacy that one element will be guaranteed to be equal to the minimum, and one element will be guaranteed to be the maximum. In these experiments, the signal variances are all assumed to be 1, meaning that the noise variances are defined by the inverse of the SNR. In order to analyze the performance of the algorithms against SNR, both the minimum and the maximum need to be considered. The expected estimation error and estimation error standard deviation are varied over SNR_{min} with a constant spread being used for SNR_{max}, more specifically, $SNR_{max,i} = \alpha + SNR_{min,i}$ for constant α.

The minimum SNR is varied over the range -30dB to 20dB, with the spread $\alpha = 5$dB for three unit power signals with bearings $[-13°, 3°, 8°]$ with sample covariance approximated over 1024 samples. The expected estimation error is shown in figure 13. The results show comparable performance from Toeplitz differencing, cumulants, and the standard algorithm with improvement from diagonal differencing, which shifted its convergence point from -4dB to -9dB. The expectation is that for larger and larger α values, the convergence of the diagonal differencing will reach and even exceed that of the standard algorithm. The results for $\alpha = 10$dB (figure 14) show the standard and diagonal differencing convergence points joining near -9dB, and at $\alpha = 40$dB (figure 15) diagonal differencing converges at -16dB to the standard algorithm's -11dB. For a single array, power disparities greater than 5dB, which is a factor of about 3, are unlikely between channels, especially given that it is likely that all channels use similar hardware components and configurations and are on reasonably close power planes. As a result it appears that for reasonable sensor channel power disparities, the diagonal differencing method as implemented here is not particularly useful in the case for which it was designed, and that the standard algorithm is still preferred. For the Toeplitz and cumulants algorithms, even for very

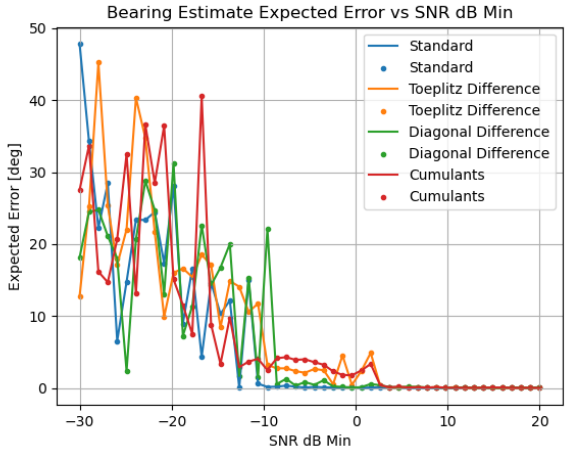

Fig. 13. Non-Uniform diagonal noise covariance expected estimation error of all algorithms vs minimum SNR with 5dB SNR spread for 1024 samples. Specifically, where SNR min is -10dB, SNR max is -5dB.

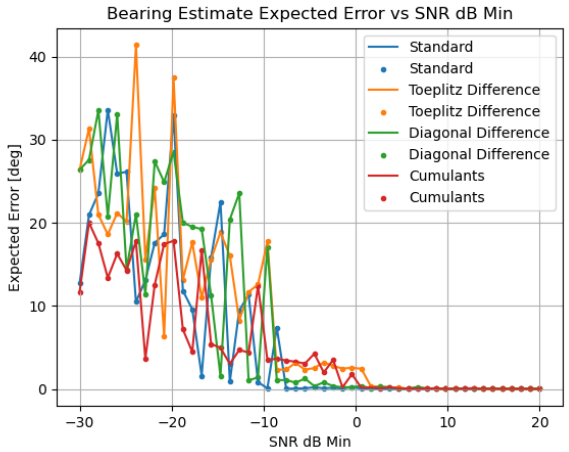

Fig. 14. Non-Uniform diagonal noise covariance expected estimation error of all algorithms vs minimum SNR with 10dB SNR spread for 1024 samples.

high noise variance spreads the convergence is marginally affected, which indicates tolerance to sensor noise power disparities, although said convergence still requires much higher SNR values than the standard algorithm.

At a 10dB SNR minimum/maximum spread, the standard and diagonal differencing algorithms are roughly equivalent in terms of convergence against minimum SNR for 1024 sample integration time. A consideration for algorithm performance at this point is required integration time to achieve convergence at this point. The expected error is analyzed against integration time (Nsamples) at -10dB minimum SNR for 10dB SNR spread in figure 16. For this configuration, the diagonal differencing algorithm requires an integration time that is a factor of 4 less than that of the standard algorithm (200 samples to 800 samples). Interestingly, the standard algorithm becomes unstable as the number of samples is increased beyond 5000, while diagonal differencing remains

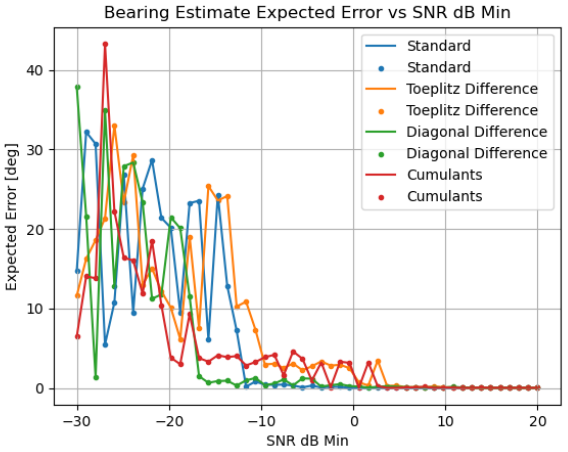

Fig. 15. Non-Uniform diagonal noise covariance expected estimation error of all algorithms vs minimum SNR with 40dB SNR spread for 1024 samples.

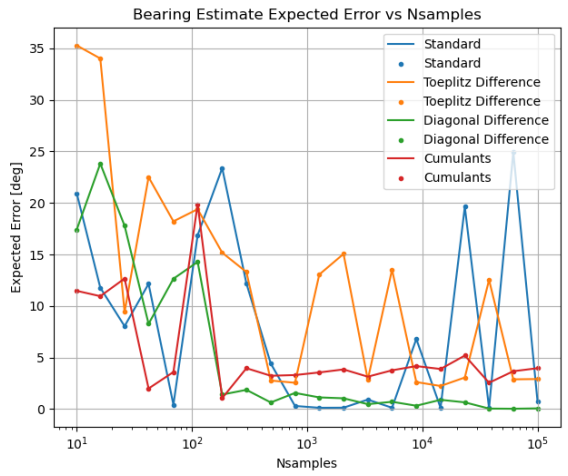

Fig. 16. Non-Uniform diagonal noise covariance expected estimation error of all algorithms vs number of samples with 10dB SNR spread for -10dB minimum SNR.

near-zero.

D. Symmetric Toeplitz Noise Covariance

The previously considered covariance structures required information only on the diagonal. This is not the case for the symmetric Toeplitz covariance, which has non-zero cross correlation terms. The off-diagonal elements are defined in terms of the correlation coefficient ρ, where $E[y_i y_j^*] = \rho_{i,j} E[y_i y_i^*] E[y_j y_j^*]$ and $-1 \leq \rho \leq 1$. There are now three parameters to consider: the minimum off-diagonal correlation coefficient ρ_{min}, the maximum off-diagonal correlation coefficient ρ_{max}, and the main diagonal elements which correspond to the noise variance that is determined directly from the SNR. Similar to the non-uniform diagonal covariance formulation, correlation coefficients ρ_{min} and ρ_{max} must appear in the matrix, and the other off-diagonals

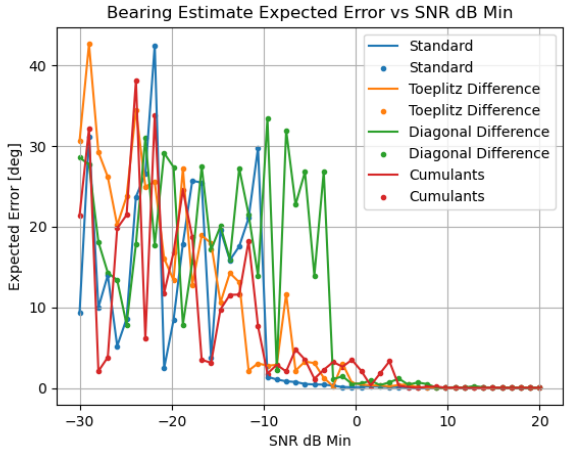

Fig. 17. Symmetric Toeplitz noise covariance expected estimation error of all algorithms vs SNR with $0 \leq \rho \leq 0.25$ for 1024 samples.

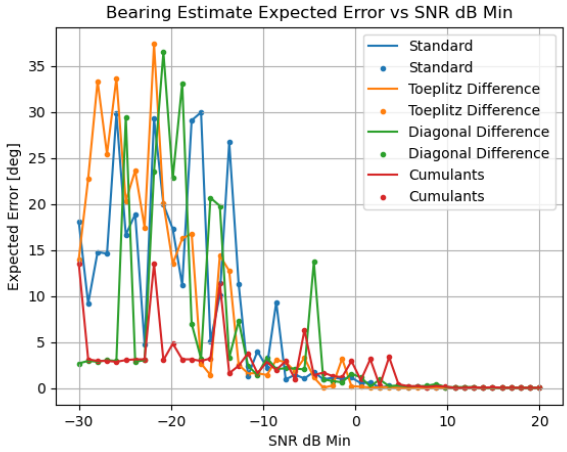

Fig. 18. Symmetric Toeplitz noise covariance expected estimation error of all algorithms vs SNR with $0.5 \leq \rho \leq 0.75$ for 1024 samples.

are determined by a random sampling from the uniform distribution on the range $[\rho_{min}, \rho_{max}]$.

When using this method to generate the covariance matrix, there is no guarantee that the resulting matrix will be positive semi-definite, so when applying equation 23 for generating noise random vectors, the square root of the eigenvalue matrix may be undefined. As such the random sampling of ρ values is repeated until a positive semi-definite matrix is generated. The expected number of iterations required to achieve a positive semi-definite matrix with this method grows exponentially with the correlation coefficient spread $\beta = \rho_{max} - \rho_{min}$, so β is typically held to 0.33 or less.

The expected estimation error is shown against SNR in figure 17, for which $0 \leq \rho \leq 0.25$ and 1024 samples were used. The results show improved convergence near -10dB for the Toeplitz differencing method, which is now somewhat comparable to the standard MUSIC algorithm, although still with greater estimation error. As compared to the uniform diagonal case, cumulants MUSIC shows minor improvements, while the diagonal differencing algorithm has marginally worse performance. When the correlation coefficient is shifted to the range $0.5 \leq \rho \leq 0.75$, all the algorithms shift to similar convergence patterns that converge with expected error between 1° and 2° near -10dB, and error less than 1° at 0dB.

Varying the minimum correlation coefficient ρ_{min} while maintaining a constant spread $\beta = 0.25$ at 0dB SNR for 1024 samples in figure 19 shows Toeplitz differencing to be the only algorithm to maintain expected error less than 2°, although all other algorithms remain close.

At 0dB SNR and $0.5 \leq \rho \leq 0.75$, the algorithms are analyzed against integration time (figure 20), again demonstrating the fluctuations out of the 2° convergence bound for most algorithms. Toeplitz differencing converges at 200 samples alongside cumulants MUSIC.

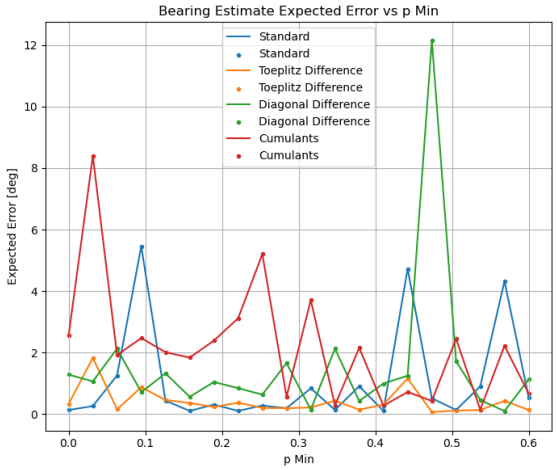

Fig. 19. Symmetric Toeplitz noise covariance expected estimation error of all algorithms vs ρ_{min} with $\rho_{max} = \rho_{min} + 0.25$ for 1024 samples at 0dB SNR.

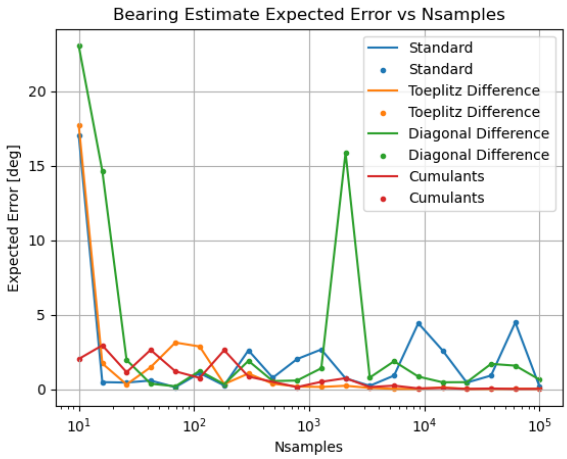

Fig. 20. Symmetric Toeplitz noise covariance expected estimation error of all algorithms vs Nsamples with $0.5 \leq \rho \leq 0.75$ at 0dB SNR.

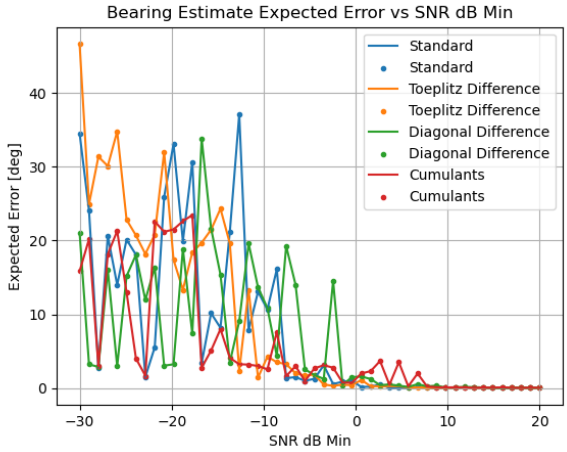

Fig. 21. Symmetric Non-Toeplitz noise covariance expected estimation error of all algorithms vs minimum SNR with $\alpha = 10$dB, $0 \leq \rho \leq 0.25$ for 1024 samples.

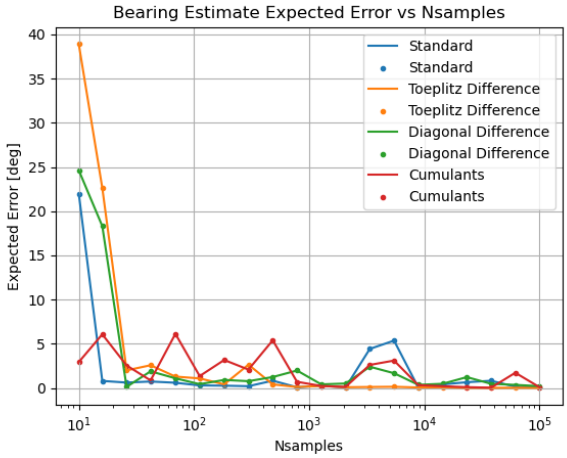

Fig. 23. Symmetric Non-Toeplitz noise covariance expected estimation error of all algorithms vs Nsamples with 0dB minimum SNR, 10dB maximum SNR and $0.5 \leq \rho \leq 0.75$.

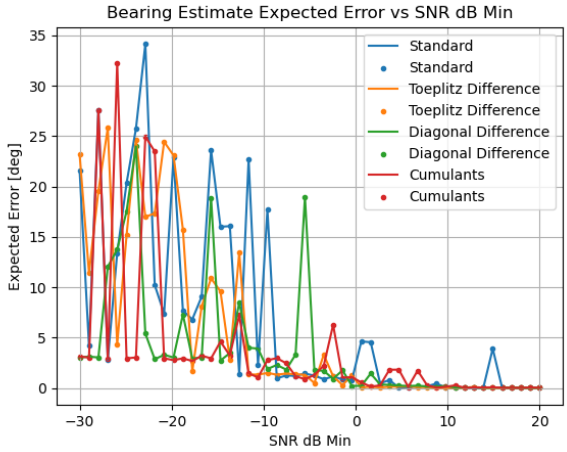

Fig. 22. Symmetric Non-Toeplitz noise covariance expected estimation error of all algorithms vs minimum SNR with $\alpha = 10$dB, $0.5 \leq \rho \leq 0.75$ for 1024 samples.

E. Symmetric Non-Toeplitz Noise Covariance

Similar to the symmetric Toeplitz structure, the symmetric non-Toeplitz structure uses $\rho_{min} \leq \rho \leq \rho_{max}$, now with the additional relaxation of the constraint that the diagonal elements must be uniform. Similar to non-uniform diagonal covariance, symmetric non-Toeplitz uses a noise variance in the range $\sigma^2_{n,min}\sigma^2_n \leq \sigma^2_{n,max}$, which is determined by the inverse of the SNR for unit-variance signals. The simulation results for various cases of ρ, SNR, and integration time are shown in figures 21, 22, and 23.

V. DISCUSSION

The standard algorithm is clearly the best performer when it comes to the ideal case of uniform diagonal noise covariance, achieving convergence at significantly lower SNR than the other algorithms and for shorter integration time. These characteristics allow it to be used in tracking weaker signals in closer to real-time, which may be vital for systems such as radar-tracking. When correlation and noise power disparities between sensors is known to be very small, the standard algorithm is the strongest choice.

When inter-sensor noise power disparities are introduced (non-uniform diagonal noise covariance), the diagonal differencing method converged at lower SNRs and for shorter integration times when the power disparity spread was greater than 10dB, however this is at best an uncommon and at worst an unrealistic expectation on real phased-array systems. For power disparities less than 10dB, the diagonal differencing approach is comparable to the standard algorithm in minimum SNR, however does improve upon the standard algorithm with a lower requisite integration time. The other algorithms minimum SNR requirement for convergence is only marginally affected as compared to the uniform diagonal case, however the required integration times increase greatly.

For correlated noise sources with uniform inter-sensor noise powers (symmetric Toeplitz), both Toeplitz differencing and cumulants saw large improvements as compared to the uniform diagonal case when correlation coefficients were large ($\rho > 0.5$), although the steady state estimation error was closer to $1.5°$ for lower SNR. A difference of $1°$ may be insignificant in many cases, but for cases in which the distance to the target sources is large it could degrade system performance. For example, consider a radar tracking system, which uses DOA estimation and the time difference between transmission and reception to localize a target which is multiple kilometers away. Estimation errors of $1°$ could yield quite large position estimation errors. The standard MUSIC algorithm only withstood a few dB of minimum SNR degradation.

For correlated noise sources with inter-sensor noise power disparities (symmetric non-Toeplitz), Toeplitz differencing and cumulants saw large improvements for the case of both small and large correlation coefficients. Again, the steady

state estimation errors remained near 1.5° for SNRs in the lower convergence region. In this case, the standard MUSIC algorithm was greatly affected when correlation coefficients were large ($\rho > 0.5$), but only marginally affected by smaller coefficients ($\rho < 0.5$).

As compared to the simulation results of the original authors of the algorithms, covariance differencing and cumulant methods did not show the improvements over the standard algorithms touted by the original authors. Further investigation into the differences between our implementation and the original authors' would be a worthwhile endeavor.

There are many intricacies to comparing DOA estimation methods which were not discussed in this paper. The signals considered were all of equal unit power and at a fixed bearing across all samples, when realistically, signal source powers and angles may ebb and flow, causing degradation of the estimation process, especially affecting the analysis which was performed against integration time. It is unrealistic to expect for any real system that a signal will remain fixed for 100,000 samples. The same angles $[-13^\circ, 3^\circ, 8^\circ]$ were considered for all experiments, expanding the study to include closer or alternatively spaced sources would give a more complete analysis. Additionally, coherency of the signal sources themselves was not considered, and has a large impact on estimation.

VI. CONCLUSION

The Multiple Signal Classification (MUSIC) algorithm is a subspace method for direction of arrival estimation using arrays of sensors. Because it depends on eigendecomposition of covariance matrices, it can be sensitive to non-idealities or unrealistic assumptions about the noise covariance structure, specifically the presence of non-white or colored noise. A handful of methods suggested by previous works [7][8][9] suggest using linear transformations of the array covariance and differencing between transformed covariance matrices to remove the effects of the non-ideal noise covariance. Another method [10][11] uses 4th order cumulants rather than covariance to ideally cancel Gaussian noise contributions entirely. This work expands on these by simulating and evaluating the performance of these methods of colored noise over varying SNR ranges, integration times, and correlation coefficient ranges under a handful of non-ideal noise covariance structures. The results indicate that for most applications, the standard algorithm is in fact the preferred method as it is the most generally well-performing, unless an unusual and specific environment is known to be present, for example a system with very high noise power disparity between sensors. Deeper analysis of the algorithms is warranted, especially with more variations related to the signal sources, including coherent signals and time-varying signals.

REFERENCES

[1] R. Schmidt, "Multiple emitter location and signal parameter estimation," in IEEE Transactions on Antennas and Propagation, vol. 34, no. 3, pp. 276-280, March 1986, doi: 10.1109/TAP.1986.1143830.

[2] Tie-Jun Shan, M. Wax and T. Kailath, "On spatial smoothing for direction-of-arrival estimation of coherent signals," in IEEE Transactions on Acoustics, Speech, and Signal Processing, vol. 33, no. 4, pp. 806-811, August 1985, doi: 10.1109/TASSP.1985.1164649.

[3] S. U. Pillai and B. H. Kwon, "Forward/backward spatial smoothing techniques for coherent signal identification," in IEEE Transactions on Acoustics, Speech, and Signal Processing, vol. 37, no. 1, pp. 8-15, Jan. 1989, doi: 10.1109/29.17496

[4] Dominic Grenier, Éloi Bossé, A new spatial smoothing scheme for direction-of-arrivals of correlated sources, Signal Processing, Volume 54, Issue 2, 1996, Pages 153-160, ISSN 0165-1684, https://doi.org/10.1016/S0165-1684(96)00104-1.

[5] Yanbo Xue, Jinkuan Wang and Zhigang Liu, "A novel improved MUSIC algorithm by wavelet denoising in spatially correlated noises," IEEE International Symposium on Communications and Information Technology, 2005. ISCIT 2005., Beijing, China, 2005, pp. 515-518, doi: 10.1109/ISCIT.2005.1566906.

[6] D. Torrieri and K. Bakhru, "The effects of nonuniform and correlated noise on superresolution algorithms," in IEEE Transactions on Antennas and Propagation, vol. 45, no. 8, pp. 1214-1218, Aug. 1997, doi: 10.1109/8.611239.

[7] A. Paulraj and T. Kailath, "Eigenstructure methods for direction of arrival estimation in the presence of unknown noise fields," in IEEE Transactions on Acoustics, Speech, and Signal Processing, vol. 34, no. 1, pp. 13-20, February 1986, doi: 10.1109/TASSP.1986.1164776

[8] S. Prasad, R. T. Williams, A. K. Mahalanabis and L. H. Sibul, "A transform-based covariance differencing approach for some classes of parameter estimation problems," in IEEE Transactions on Acoustics, Speech, and Signal Processing, vol. 36, no. 5, pp. 631-641, May 1988, doi: 10.1109/29.1573.

[9] A. Moghaddamjoo, "Transform-based covariance differencing approach to the array with spatially nonstationary noise," in IEEE Transactions on Signal Processing, vol. 39, no. 1, pp. 219-221, Jan. 1991, doi: 10.1109/78.80789.

[10] B. Porat and B. Friedlander, "Direction finding algorithms based on high-order statistics," in IEEE Transactions on Signal Processing, vol. 39, no. 9, pp. 2016-2024, Sept. 1991, doi: 10.1109/78.134434.

[11] M. C. Dogan and J. M. Mendel, "Applications of cumulants to array processing. II. Non-Gaussian noise suppression," in IEEE Transactions on Signal Processing, vol. 43, no. 7, pp. 1663-1676, July 1995, doi: 10.1109/78.398727.

[12] N. Bienert, "Lecture 6", Stochastic and Environmental Signal Processing, ECEN 5244, University of Colorado at Boulder, pp. 4-8, September 2024.

[13] N. Golding, MUSIC DOA Analyzer. [Online]. Available: https://github.com/NateGolding/ECEN5244_Project

[14] Harris, C.R., Millman, K.J., van der Walt, S.J. et al. Array programming with NumPy. Nature 585, 357–362 (2020). DOI: 10.1038/s41586-020-2649-2.

[15] Pauli Virtanen, Ralf Gommers, Travis E. Oliphant, Matt Haberland, Tyler Reddy, David Cournapeau, Evgeni Burovski, Pearu Peterson, Warren Weckesser, Jonathan Bright, Stéfan J. van der Walt, Matthew Brett, Joshua Wilson, K. Jarrod Millman, Nikolay Mayorov, Andrew R. J. Nelson, Eric Jones, Robert Kern, Eric Larson, CJ Carey, İlhan Polat, Yu Feng, Eric W. Moore, Jake VanderPlas, Denis Laxalde, Josef Perktold, Robert Cimrman, Ian Henriksen, E.A. Quintero, Charles R Harris, Anne M. Archibald, Antônio H. Ribeiro, Fabian Pedregosa, Paul van Mulbregt, and SciPy 1.0 Contributors. (2020) SciPy 1.0: Fundamental Algorithms for Scientific Computing in Python. Nature Methods, 17(3), 261-272. DOI: 10.1038/s41592-019-0686-2.

[16] J. D. Hunter, "Matplotlib: A 2D Graphics Environment", Computing in Science & Engineering, vol. 9, no. 3, pp. 90-95, 2007.